Calhoun
Institutional Archive of the Naval Postgraduate School

Calhoun: The NPS Institutional Archive

DSpace Repository

Theses and Dissertations | 1. Thesis and Dissertation Collection, all items

1951

Resonances in the C [Superscript 14] (p,n) N [Superscript 14] reaction and energy levels of N [Superscript 15].

Roseborough, William Daniel

Massachusetts Institute of Technology

http://hdl.handle.net/10945/14562

Downloaded from NPS Archive: Calhoun

DUDLEY KNOX LIBRARY

http://www.nps.edu/library

Calhoun is the Naval Postgraduate School's public access digital repository for research materials and institutional publications created by the NPS community. Calhoun is named for Professor of Mathematics Guy K. Calhoun, NPS's first appointed -- and published -- scholarly author.

Dudley Knox Library / Naval Postgraduate School
411 Dyer Road / 1 University Circle
Monterey, California USA 93943

RESONANCES IN THE $C^{14}(p,\alpha)N^{14}$ REACTION AND ENERGY LEVELS OF N^{15}

WILLIAM DANIEL ROSEBOROUGH, JR.

Library
U. S. Naval Postgraduate School
Monterey, California

Plant 220
8854

RESONANCES IN THE $C^{14}(p,n)N^{14}$ REACTION

AND

ENERGY LEVELS OF N^{15}

by

WILLIAM DANIEL ROSEBOROUGH, JR.

Commander, U.S. Navy

B.S., United States Naval Academy
(1940)

M.S., Massachusetts Institute of Technology
(1945)

SUBMITTED IN PARTIAL FULFILLMENT OF THE

REQUIREMENTS FOR THE DEGREE OF

MASTER OF SCIENCE IN PHYSICS

Resonances in the $C^{14}(p,n)N^{14}$ Reaction And Energy Levels of N^{15}

by

William Daniel Roseborough, Jr.
Commander, U.S. Navy

Submitted for the degree of Master of Science
in the Department of Physics on July 1,1951

ABSTRACT

The Rockefeller Electrostatic Generator at M.I.T. was used as a source of protons for a study of the (p,n) reaction on C^{14}. Two 3 Kev and one 8 Kev targets were employed. The Rockefeller Generator is equipped with nuclear resonance control of the analyzing magnetic field for determining and controlling the proton beam energy. A long counter was used for neutron detection. Nine resonances were found in the proton energy range between 1.180 Mev and 3.125 Mev, at 1.165, 1.310, 1.664, 1.789, 1.883, 2.024, 2.079, 2.272, and 2.451 Mev. The proton energy, neutron yield, resonance width at half-maximum, and target thickness of each resonance are tabulated. A partial energy level structure of N^{15} in the region between approximately 11 to 12.5 Mev above the ground state is compared with the level structure obtained from other sources.

TABLE OF CONTENTS

	Page
ABSTRACT	1
LIST OF FIGURES	iii
LIST OF TABLES	iv
CHAPTER I - INTRODUCTION	1
CHAPTER II - DESCRIPTION OF APPARATUS AND TARGET PREPARATION	10
CHAPTER III - EXPERIMENTAL PROCEDURE	28
CHAPTER IV - EXPERIMENTAL RESULTS	31
A. Unenriched Sodium Cyanide Target	31
B. First Enriched Sodium Cyanide Target	34
C. Second Enriched Sodium Cyanide Target	39
D. Third Enriched Sodium Cyanide Target	47
CHAPTER V - CONCLUSIONS	57
BIBLIOGRAPHY	62
ACKNOWLEDGMENTS	64
APPENDIX A - Table V - Conversion of Frequency to Energy-Kc/Kev	66
APPENDIX B - Figure 15 - Proton Energy Loss Per Unit Target Thickness vs Proton Energy	67
APPENDIX C - Magnetic Field Regulation Using Nuclear Magnetic Resonance	68

LIST OF FIGURES

Page

Figure 1 - Rockefeller Electrostatic Generator with Pressure Tank Removed 12

Figure 2 - Rockefeller Electrostatic Generator Cross-Sectional Drawing 14

Figure 3 - Experimental Set-up Showing Analyzing Magnet, Rotating Target Holder, Target, and Long Counter 16

Figure 4 - Rockefeller Generator Control Console . 18

Figure 5 - Rockefeller Generator Control Console Showing Nuclear Resonance Control Frequency Meter 20

Figure 6 - Cross-Sectional Sketch of the Long Counter 25

Figure 7 - Neutron Yield from the $Li^{7}(p,n)Be^{7}$ and $C^{13}(p,n)N^{13}$ Reactions 33

Figure 8 - Neutron Yield from the $C^{14}(p,n)N^{14}$ Reaction with Cl^{37} Contamination vs. Proton Energies of 0.975 Mev to 2.200 Mev. First Enriched NaCN Target 36

Figure 9 - Neutron Yield from the $C^{14}(p,n)N^{14}$ Reaction with Cl^{37} Contaminant vs. Proton Energies of 1.155 Mev to 1.175 Mev and 1.870 Mev to 2.150 Mev. First Enriched NaCN Target 41

Figure 10 - Neutron Yield from the $C^{14}(p,n)N^{14}$ Reaction vs. Proton Energies of 1.06 Mev to 2.45 Mev. Second Enriched NaCN Target. 43

Figure 11 - Neutron Yield from the $C^{14}(p,n)N^{14}$ Reaction in Vicinity of Resonances whose Maximum Values occur at 1.165 Mev and 1.310 Mev. Second Enriched NaCN Target . 46

Figure 12 - Neutron Yield from the $C^{14}(p,n)N^{14}$ Reaction vs. Proton Energy of 1.15 Mev to 2.60 Mev. Third Enriched NaCN Target . 49

Figure 13 - Neutron Yield from the $C^{14}(p,n)N^{14}$ Reaction vs. Proton Energy of 1.950 Mev to 2.200 Mev. Third Enriched NaCN Target. 52

LIST OF FIGURES (continued)

Page

Figure 14 - Partial Energy Level Diagram for N^{15} .. 61

Figure 15 - Proton Energy Loss per Unit Target Thickness vs. Proton Energy 67

LIST OF TABLES

		Page
Table I -	Positions of Resonances in the $C^{14}(p,n)N^{14}$ Reaction expressed in terms of Proton Energies in Kev	8
Table II -	Proton Energy, neutron yield, Target Thickness, and width at half-maximum amplitude of resonances found in the third enriched NaCN Target	55
Table III -	Calculation of Target Thickness and Resonance Widths at half-maximum	56
Table IV -	Positions of Resonances in the $C^{14}(n,p)N^{14}$ Reactions Expressed in terms of Proton Energies in Kev	59
Table V -	Conversion Factors for Converting Proton Energies, Kilocycles to Kev	66

CHAPTER I

INTRODUCTION

The interaction of nuclear particles with nuclei is being used extensively in the study of the structure of nuclei. Based on Bohr's hypothesis[a] nuclear reaction usually can be considered as taking place in two steps. The bombarding particle combines with a nucleus to form an excited compound nucleus which then decays either by the emission of a particle or a gamma ray. In the work reported here, a proton combines with the C^{14} nucleus to form an excited state of N^{15} which subsequently disintegrates into N^{14} in the ground state with the emission of a neutron. The cross-section for the formation of the compound nucleus is given by Blatt and Weisskopf (Bl50) as:

$$(1) \quad \sigma_c^{\ell} = (2\ell + 1)\, \pi \lambda_p^2\, T_p^{\ell}$$

where ℓ is the angular momentum of the bombarding proton, and T_p^{ℓ} is the transmission coefficient of the nuclear surface for the proton. The transmission coefficient, T_p^{ℓ}, gives the percentage of protons incident upon the nucleus which will penetrate the potential barrier. The computation of the values of T_p^{ℓ} for protons is quite complicated but is given in some detail in (Bl50). For the present we consider only that T_p^{ℓ} is largest for small values of ℓ and decreases rapidly as ℓ increases.

The potential barrier surrounding a nucleus for a particle of mass m is given by Blatt and Weisskopf (Bl50) as:

$$(2)\quad U_{\ell}(r) = V(r) + \frac{\hbar^2 \ell(\ell+1)}{2mr^2} \quad \text{where}$$

V(r) is the coulomb potential at a distance (r) from the center of the nucleus, and

$\frac{\hbar^2 \ell(\ell+1)}{2mr^2}$ is the centrifugal potential.

The "centrifugal" potential appears in the wave equation reduced to one-dimensional form and is a fictitious mathematical contribution to the potential barrier for particles which do not make head-on collisions with the nucleus. It should be noted that the "centrifugal" potential is zero for protons with $\ell = 0$, and the potential barrier for such protons is merely the coulomb potential. The coulomb potential of C^{14} is computed to be 2.38 Mev using equation (3) and taking the nuclear radius $R = 1.5(10^{-13})A^{1/3}$ where A = atomic weight and Z = atomic number of the bombarded nucleus.

$$(3)\quad V(r) = \frac{Zze^2}{R} = \frac{6(1)(4.8 \times 10^{-10})^2}{1.5(10)^{-13}A^{1/3}} = 3.82\ (10)^{-6}\ \text{ergs}$$

$$= 2.38\ \text{Mev.}$$

Bombarding protons (Z = 1) of energies up to 3.5 Mev were used in these experiments. Quantum mechanically low energy protons (2.38 Mev) have a small but finite probability of penetration which increases exponentially with increase in the

energy of the proton. The energy ranges for which this is true depend on both the height and thickness of the potential barrier. Since there is no coulomb barrier for the emission of neutrons from the compound nucleus, the barrier penetration factor, T_n^{ℓ}, will be a function only of the "centrifugal" barrier which varies with the angular momentum of the neutrons in the following manner:

ℓ	T_n^{ℓ}
0	$T^0 = 1$
1	$T^1 = \dfrac{x^2}{1 + x^2}$
2	$T^2 = \dfrac{x^4}{9 + 3x^2 + x^4}$

where $x = \dfrac{R}{\lambda\!\!\!^{-}_n}$, R being the nuclear radius given above and being the de Broglie wave length of the emitted neutron divided by 2π. Since there is no "centrifugal" barrier for $\ell = 0$ neutrons, the cross-section for the (p,n) reaction is approximately equal to the cross-section for the formation of the compound nucleus (given on page 1), provided neutron emission is energetically possible, i.e., the bombarding proton has an energy greater than the (p,n) threshold energy for the target nucleus.

Were it not for the effect of resonances the cross-section for the (p,n) reaction would be the product of the cross-section for the formation of the compound nucleus, equation (1), and

the cross-section for the emission of a neutron of which T_n^ℓ forms a part. The familiar Breit-Wigner relation expresses this over-all cross-section as shown in equation (4):

$$(4) \quad \sigma = \pi \lambda\!\!\!^{-2} (2\ell + 1)\, G_J^\ell \frac{\Gamma_p^\ell \Gamma_n}{(E-E_R)^2 + \frac{\Gamma^2}{4}} \quad \text{where}$$

$\lambda\!\!\!^{-} = \frac{h}{2\pi m v}$ where m is the mass and v the velocity of the incident proton in the center of mass system.

Γ_p^ℓ is the half-width for emission of a proton of angular momentum ℓ from the compound nucleus.

Γ_n is the half-width for emission of a neutron, of any possible angular momentum or energy.

Γ is the total level width, the sum of the partial widths of all processes by which the compound nucleus can decay.

G_J^ℓ is a statistical weight factor.

The application of the Breit-Wigner relation to the experimental results contained in this thesis is the subject of an intensive study now in progress by other members of the Nuclear Shielding Group. As a result of this study, it may be possible to assign ℓ-values to all of the observed resonances. However this is not possible at the present time. This thesis summarizes the experimental procedure and the experimental results obtained, but gives only a very general consideration to the theoretical aspects of the problem.

PREVIOUS INVESTIGATIONS

Shoupp, Jennings and Sun (Sh48), in 1947, investigated

the threshold and resonances in the $C^{14}(p,n)N^{14}$ reaction and the energy levels of N^{15}. This reaction is the inverse of the $N^{14}(n,p)C^{14}$ process investigated by Barschall and Battat in 1946 (Ba46), Hughes and Eggler in 1948 (Hu48), Stebler and Huber in 1948 (St48), and Johnson and Barschall in 1950 (Jo50).

The energy levels of N^{15} determined by these previous investigations were not in very good agreement. The threshold of the $C^{14}(p,n)N^{14}$ reaction was found by Shoupp et al. to be 0.664 ± .009 Mev. They used a thick C^{14} target, a one-millimeter layer of $BaCO_3$ powder containing 2.7 percent of C^{14}. The threshold energy was determined by extrapolating the excitation function to the threshold by a method based on a yield equation developed by Stephens, Spruch, and Schiff (St47), whose work indicates that the neutron yield near the threshold should vary directly with $(E_p - E_t)^{3/2}$, where E_p is the proton energy and E_t the threshold energy. This theoretical relationship involves the assumptions that the reverse process, the capture of a slow neutron by N^{14}, obeys a 1/v law and that no resonances exist near the threshold. Subsequently Tollestrup et al. (To50) have calculated the value of the $C^{14}(p,n)N^{14}$ threshold to be E_t = 671 Kev based on the best measured value of Q (626 Kev) from nuclear reactions and mass spectrographic measurements. This value of E_t is used in this work.

Shoupp et al. used also a thin C^{14} target to determine the resonances in the $C^{14}(p,n)N^{14}$ reaction. This target was prepared by allowing CO_2 containing C^{14} to react with a very

thin layer of $Ba(OH)_2$ which had been sprayed on a tantalum plate. This reaction produced a small amount of $BaCO_3$ containing C^{14}. The beta activity was found to be 0.26 microcurie per cm^2. About 2.7 percent of the carbon atoms were C^{14} and the thickness of the $BaCO_3$ was about $6(10)^{-6}$ cm. They estimated a target thickness of 3 Kev at a proton energy of 1.14 Mev. This estimate of target thickness is questionable. The measurement of the C^{14} radioactivity to determine the amount of C^{14} in the target is subject to considerable error. It is doubtful that the layer of $Ba(OH)_2$ which was sprayed on the tantalum backing plate was of uniform thickness, but was more probably a non-uniform crystalline surface. There is also considerable doubt that all of the $Ba(OH)_2$ was converted to $BaCO_3$ which would result in a thicker target than indicated by the C^{14} radioactivity. They observed strong resonances at 1.14, 1.30, and 2.05 Mev and doubtful ones at 1.47, 2.21, and 2.65 Mev. The confirmation of the doubtful resonances was impossible because of the lack of resolution of their experimental method. This lack of resolution is discussed in Chapter IV, "Experimental Results." They calculated the cross-section of the process to be about 0.7 barn for the top of the first resonance.

The following reactions are known to occur in nitrogen under bombardment by fast neutrons:

$$_7N^{14} + n \longrightarrow {}_6C^{14} + p + Q_1$$

$$_7N^{14} + n \longrightarrow {}_5B^{11} + \alpha + Q_2 .$$

Using neutrons from the $Li^{7}(p,n)Be^{7}$ reaction, Barschall and Battat (Ba46) measured the cross-sections of these reactions for neutrons of energies between 200 and 1700 Kev. They observed resonances for neutron energies of 550, 700, and 1450 Kev.

Stebler and Huber in 1948 observed resonances for the $N^{14}(n,p)C^{14}$ reaction for neutrons of 480, 640, and 1410 Kev, and for the $N^{14}(n,\alpha)B^{11}$ reaction for neutrons of 1410 and 1770 Kev.

More recently, Johnson and Barschall measured the cross-sections for the reactions $N^{14}(n,p)C^{14}$ and $N^{14}(n,\alpha)B^{11}$ for neutron energies from 150 to 2100 Kev. Resonances for the (n,p) reaction were found at 499, 640, 993, and 1415 Kev, and for the (n,α) reaction at 1415 and 1800 Kev.

The positions of these resonances are tabulated in Table I for ready comparison.

Malm and Buechner (Ma50) in 1950 investigated the $N^{14}(d,p)N^{15}$ reaction with 1.4 Mev deuterons. The protons from the reaction were analyzed into energy groups by a high-resolution magnetic spectrometer. Their trajectories were located by ascertaining where they struck a nuclear track plate located in the annular gap of a large annular magnet in a position diametrically opposite to that of the target. Several groups of protons appeared, each characterized by a specific energy. The differences in proton energy correspond to differences in the excitation energy of the residual nucleus, N^{15},

TABLE I

Positions of Resonance Peaks in the $C^{14}(p,n)N^{14}$ Reaction Expressed in Terms of Proton Energies, E_p, in Kev. $E_p = E_n + E_t = E_n + .671$ Kev.

(Resonances reported as doubtful are enclosed by parenthesis).

Shoupp et al. (Sh48)	Johnson and Barschall (Jo50)		Stebler and Huber (St48)		Barschall and Battat (Ba46)	
E_p	E_n	E_n+671	E_n	E_n+671	E_n	E_n+671
1140 ± 20	499 ± 5	1170 ± 5	480 ± 50	1151 ± 50	550	1221
1300 ± 20	640 ± 7	1311 ± 7	640 ± 40	1311 ± 40	700	1371
(1470 ± 50)						
	(993 ± 12)	(1664 ± 12)				
2050 ± 20	1415 ± 50	2086 ± 50	1410 ± 90	2081 ± 90	1450	2121
(2210 ± 50)						
	1800 ± 15	2471 ± 15	1770 ± 110	2441 ± 110		
(2650 ± 50)						

and energy levels of this nucleus were determined at 5.276, 5.305, 6.328, 7.164, 7.309, 8.315 Mev, all $\pm$ 0.006 Mev. They also discussed similar work by Guggenheimer, Heitler and Powell (Gu47) and Wyly (Wy49), and the $N^{14}(n,\gamma)N^{15}$ work by Kinsey, Bartholomew, and Walker (Ki50).

It has been generally assumed in the concept of the compound nucleus that the energy levels of a nucleus are the same, regardless of the process by which the nuclide is formed. However, an insufficient number of nuclei formed by two or more different processes have been studied to establish beyond question the validity of this theory. Since the reported energy levels of N^{15} formed by the two processes

$$C^{14} + p \longrightarrow N^{15*} \longrightarrow N^{14} + n$$

$$N^{14} + n \longrightarrow N^{15*} \longrightarrow C^{14} + p$$

were not in very good agreement, it was considered worthwhile to restudy them with the greater resolution available with the Rockefeller electrostatic generator equipped with the nuclear resonance control of the analyzing magnetic field. The experiments on the first process are reported in this work. The second process was studied concurrently here at M.I.T. by Hinchey and Stelson (Hi51) and their results along with those of these experiments are listed in Table IV, Chapter V. The energy levels of N^{15} found in these two experiments are in excellent agreement and indicate the existence of three levels not previously reported.

CHAPTER II

APPARATUS AND TARGET PREPARATION

The Rockefeller Electrostatic Generator is an almost ideal source of monoenergetic protons or deuterons in the energy range of approximately 0.5 - 4.0 Mev as bombarding particles for nuclear reactions. The principles of the generator have been discussed in detail by Van de Graaff and others (Va31), (Va33), (Va48), (Tu35), and (He37). A photograph of the Rockefeller generator with the pressure tank removed is shown in Figure 1. A cross-sectional sketch of the generator is shown in Figure 2. The experimental set-up showing the proton beam analyzing magnet, rotating target holder, target, and long counter is shown in Figure 3. The center and right-hand sections of the generator control console are shown in Figure 4. The center and left-hand sections of the generator control console, showing the nuclear resonance control frequency meter, are shown in Figure 5. This discussion is limited to the energy, intensity, focus, analysis, resolution, and stability of the protons used in this experiment.

The maximum voltage attainable is dictated by the dielectric strength of the insulating gas and the breakdown voltage of the column and tube insulation. The maximum voltage obtained at the time of these experiments was 3.5 Mev. However, the generator has been on occasion operated at + 4.2 Mev. A

Figure 1

ROCKEFELLER ELECTROSTATIC GENERATOR WITH

PRESSURE TANK REMOVED

(This photograph was taken prior to the installation of the positive ion source and accelerator tube)

Figure 2

ROCKEFELLER ELECTROSTATIC GENERATOR

CROSS-SECTIONAL DRAWING

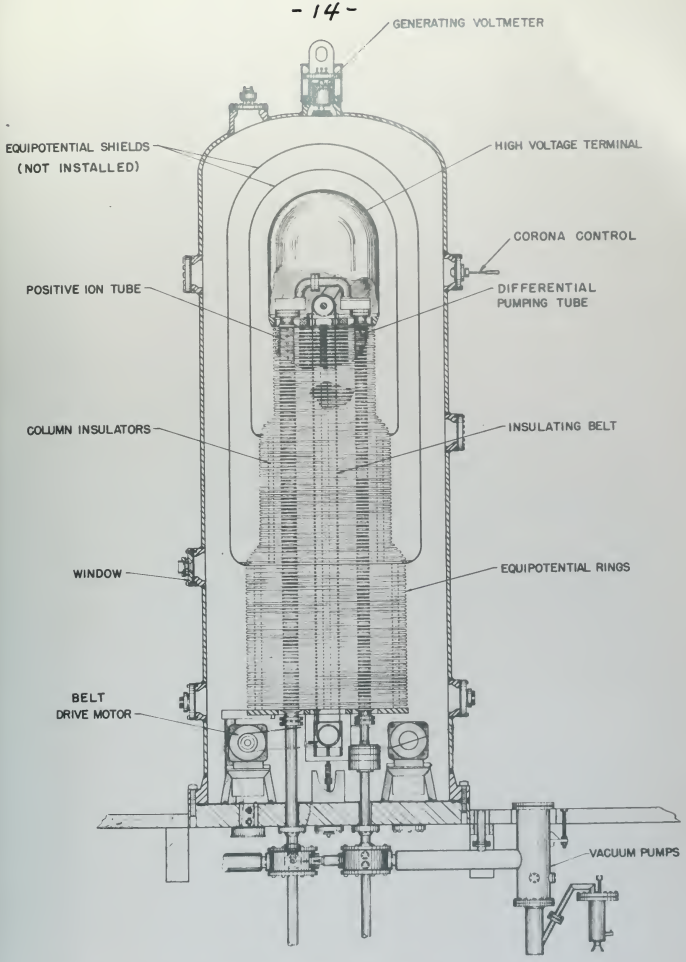

HIGH VOLTAGE GENERATOR FOR NUCLEAR RESEARCH

6 12 18
ALE IN INCHES

MASS INST OF TECH
HIGH VOLTAGE LAB
BUILDING 46

Figure 3

EXPERIMENTAL SET-UP SHOWING

(1) ANALYZING MAGNET, (2) ROTATING TARGET HOLDER,

(3) TARGET, and (4) LONG COUNTER.

The long counter has been moved away from the target sufficiently to permit a view of the target.

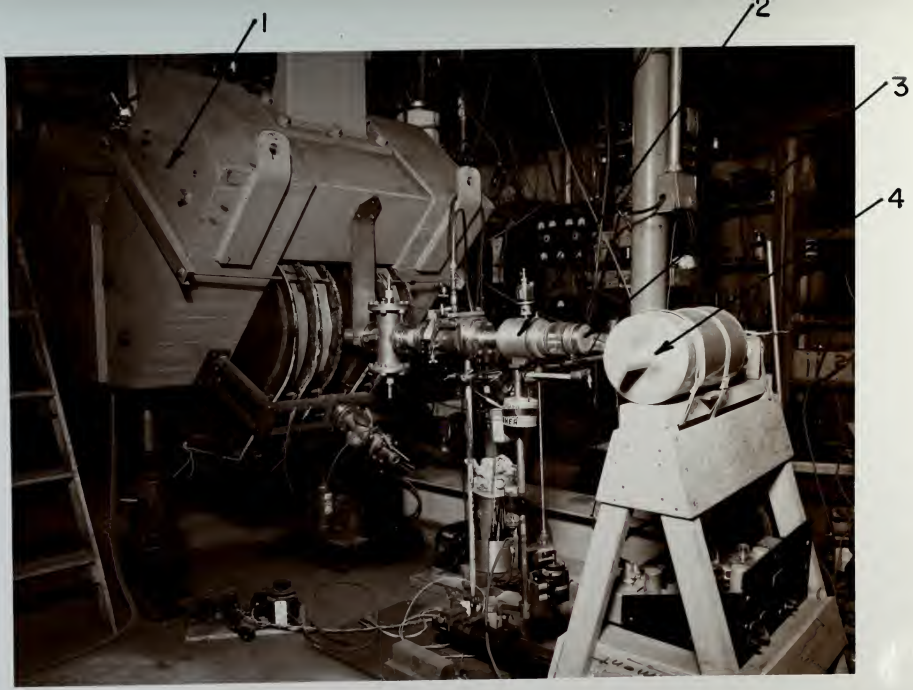
1
2
3
4

Figure 4

ROCKEFELLER GENERATOR CONTROL CONSOLE

Proton Beam Microammeter shown on top of central section.

Figure 5

ROCKEFELLER GENERATOR CONTROL CONSOLE SHOWING NUCLEAR RESONANCE CONTROL FREQUENCY METER

The General Radio Co. Model LR-3 Combined Heterodyne Frequency Meter and Crystal Controlled Calibrator Equipment having an accuracy of 1 part in 100,000 is shown on the table to the left of the console, and was used in these experiments.

46-117
LABORATORY NO. 2

radio frequency ion source is used. The protons are ejected into the accelerating tube by a repeller electrode. A maximum current of about 20 microamperes of analyzed protons can be obtained.

The ion beam from the source is focused by a lens of adjustable voltage (50 Kev max.) located below the source orifice. At the lower end of the accelerating tube are two pair of adjustable entrance slits which limit the size of the beam passing through. A set of sixteen deflection rods, spaced at 22 1/2° intervals, is mounted inside the accelerating tube extension and connected to two D.C. voltage supplies. The rods are connected together by resistors, and the voltages applied to rods 90° apart form a directional field which maintains the beam in the center of the slits.

The beam then passes through an analyzing magnetic field which deflects it through an angle of 90°. At the end of the analyzing chamber, the beam is again limited in cross-section by a pair of insulated exit slits. Whenever the beam is not centered on the exit slits a voltage differential exists across the slits, and this voltage is amplified electronically and used for voltage stabilization. The beam entering the deflection chamber in the magnetic field passes through the entrance slits which are usually set at an opening of about 1 cm. x 1 mm. With an exit slit 1 mm. wide, the size of the spot on the target is about 1.5 mm. x 1.5 mm., and the energy spread of the proton beam is of the order of 300 volts.

The magnetic analyzing field is stabilized to about .005% by the nuclear resonance method. This method allows readings to be taken at intervals of about 0.2 kilovolt. Since the nuclear resonance frequency is proportional to the magnetic field, this device may be used as a measure of the magnetic field, and therefore of the energy of the proton beam. The energy of the beam is proportional to the square of the frequency, eg, $E = kf^2$. The proportionality constant, k, was calculated from the Li^7 threshold (determined by Herb (He49) to be 1.8822 Mev). The frequency corresponding to this energy is 10.485 mc. Therefore:

$$k = \frac{E_o}{f_o^2} = \frac{1.8822}{(10.485)^2} = 0.017121 \frac{Mev}{(mc)^2} = 17.121 \frac{Kev}{(mc)^2} .$$

This value of k was used in these experiments. The accuracy of the measured value of the energy of the beam is limited by the variation of the value of k with energy (<.02%), the accuracy of the frequency measurement (.002%), the width of the beam-defining slits (.15% for 1 mm. slits, .075% for 0.5 mm. slits), the possible error in the value of k due to the uncertainty in our determination of the Li^7 threshold (0.1%), a drift in the value of k between calibrations (0.05%), and the use of the non-relativistic equations used in the derivation of the frequency-energy relationship (<0.05%). The magnitudes of these errors are discussed in greater detail by Schoenfeld and Duborg (Sc51). They estimated that the energies of the proton

beams are accurate to within 0.1%, relative to Herb's measured value of the $Li^7(p,n)$ threshold. A discussion of the principle and operation of the nuclear resonance magnet control is given in Appendix C.

The generator voltage is stabilized by means of the corona current to an assembly of seven sharp points located near the high voltage terminal. The voltage differential existing across the exit slits is transmitted electronically to the corona control system so that the beam remains on the target at the energy determined by the magnetic field.

The neutron yield was measured by a long counter which is similar to the one described by Hanson and McKibben (Ha47). This counter operates on the principle that neutrons striking the paraffin layer surrounding the enriched BF_3 counter will be slowed down so that the sensitivity of the device will be relatively independent of the energy of the incident neutrons. The geometry of the long counter used in this experiment is shown in Figure 6. Willard (Wi50) determined that the relative sensitivity of this counter increased from 0.9 at a neutron energy of 0.1 Mev to 1.0 at 1 Mev and remained constant to the maximum neutron energy obtained. This sensitivity was obtained with the counter axis parallel to the proton beam. Although it is not known how the sensitivity varies when the axis of the counter is perpendicular to the proton beam (as used in the present work), such knowledge is not essential for the purpose of this experiment. The counter was placed as close to the target as practicable (3 cm.) in order to subtend as large a solid

Figure 6

CROSS-SECTIONAL SKETCH OF THE LONG COUNTER

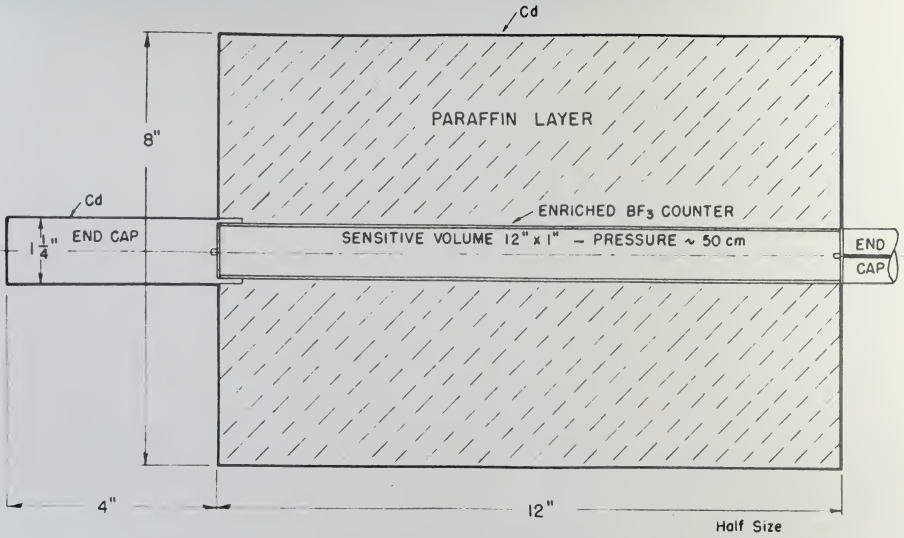

LONG COUNTER

angle as possible.

The pulses obtained from the long counter were amplified by a Model 101 preamplifier and Model 100 amplifier (E149) feeding into an Atomic Instrument Company scaler. The voltage of the center wire was maintained at 2240 volts. The counter was checked frequently against a 1 mg. radium-berylium neutron source.

The targets used in this experiment were prepared by Baird Associates of Cambridge, Massachusetts, by evaporation in vacuo of NaCN placed in a tantalum boat onto a tantalum backing plate. A thin target prepared from ordinary NaCN was obtained initially and bombarded at considerable length to determine the durability of the target. The neutron yield from a trace of lithium in the target remained constant during a bombardment of several hours, therefore the target preparation method appeared to be satisfactory and authority was obtained from the Isotopes Division of the A.E.C. at the Oak Ridge National Laboratory to purchase two millicurie of C^{14} in the form of NaCN from Tracerlab, Inc.

A thin target of NaCN enriched in C^{14} was obtained. Upon bombarding this target with protons of energy up to about 2.5 Mev, it was found that the target was contaminated with chlorine. The thickness of the target was estimated to be 3 Kev based on the width at half-maximum of a well-defined chlorine resonance.

Tracerlab, Inc. then attempted to eliminate the chlorine

contamination. A supply of NaCN containing ordinary carbon which had been deliberately contaminated with chlorine and then purified was obtained and a thin target prepared. A test run indicated that the chlorine contamination had been successfully eliminated, and a purified supply of NaCN containing C^{14} was obtained and a second thin target of enriched NaCN was procured from Baird Associates and bombarded. A final run was made with a third enriched target, thicker than the first two, to get a neutron yield that was well above the background.

CHAPTER III

EXPERIMENTAL PROCEDURE

The target was mounted in a rotating target holder eccentric to the proton beam. The long counter was placed at a distance of 3 cm. from the target with the axis of the counter horizontal and perpendicular to the proton beam. In this position the counter subtended a vertical arc of 106° and a horizontal arc of 169°. Since the C^{14} enrichment of the NaCN was quite small (approximately 0.55% of the NaCN target atoms were C^{14} atoms) it was considered necessary to place the counter as close to the target as practicable in order to obtain a reasonable counting rate. For a 3 Kev (6×10^{-6} cm) target, and using the 0.7 barn cross-section estimated by Shoupp et al. for the 1.14 Mev resonance, a maximum yield of 7.5 $(10)^3$ neutrons per microampere of protons is estimated.

For $\ell = 0$ protons the neutron yield will be isotropic in the center of mass system and slightly forward in the laboratory system. For $\ell > 0$ protons the distribution is not known, nor was it determined in these experiments, but is is probably anisotropic.

Hanson and McKibben (Ha47) found the absolute sensitivity of the long counter to be such that it would give about 1 count for every 10^5 neutrons emitted from a source placed at a distance of 1 meter from the front face of the counter. The counter used in these experiments differed from that of Hanson and McKibben in that the paraffin had a covering of

cadmium to absorb incident thermal neutrons therby reducing the background. The absolute sensitivity of the long counter used in these experiments was not determined.

It is understood that compounds containing a much greater enrichment of C^{14} will soon be available from Oak Ridge. A target with a larger percentage of C^{14} atoms would provide sufficient neutron yield to permit locating the counter axially with respect to the proton beam and at a greater distance from the target. It may also be possible to study the angular distribution of the neutron yield.

The operation of the long counter, amplifiers, and scaler was checked before and after each run by means of a radium-beryllium neutron source. A proton beam of 3 to 7 microamperes from the Rockefeller generator was directed onto the target. The proton energy was set and held constant by means of the nuclear resonance magnet control while the neutron yield for a given number of protons was obtained. The number of protons was indicated by the beam current integrator, 400 microcoulombs being used at each energy. In general the neutron yields were obtained at energy intervals corresponding to 10 Kc on the nuclear resonance frequency control (i.e., about 2.6 Kev at 1 Mev energy and about 4.5 Kev at 3 Mev energy). In the vicinity of resonances, or suspected resonances, the intervals were reduced to 5 Kc or less. The conversion factor of Kc to Kev was determined from Table V in the Appendix.

The neutron background was obtained by bombarding a plain

tantalum target over the same proton energy range in the first series of runs. In the runs made with the purified NaCN target, the background was obtained during the runs by periodically closing the flap valve just ahead of the target, thus preventing the proton beam from impinging on the target. Since the beam current integrator was inoperative with the flap valve closed, the average time required for 400 micro-coulomb counts was used as the timing interval.

CHAPTER IV

EXPERIMENTAL RESULTS

Unenriched Sodium Cyanide Target.

This thin target, prepared by Baird Associates by evaporating ordinary sodium cyanide in vacuo onto a tantalum backing plate, was used to determine whether the carbon would stay in place under prolonged bombardment with protons. Adamson (Ad50) had found it necessary to deposit a thin layer of gold over the cyanide to prevent volatilization.

The plot of the neutron counts per microcoulomb for this target, Figure 7, showed a threshold at a proton energy of about 1.88 Mev and a resonance at about 2.26 Mev, both characteristic of Li^{7}. In addition the C^{13} threshold at about 3.26 Mev found by Adamson (Ad50) was also observed. Sustained bombardment at proton currents up to 10 microamperes proved that the method of target preparation was satisfactory, that the carbon would stay in place under prolonged bombardment, and that the gold foil cover used by Adamson was not required for this target. Over a period of several hours bombardment the neutron yield for a given proton energy decreased but slightly.

The lithium contamination occurred in the target preparation as lithium targets had been prepared in the evaporation apparatus immediately preceeding the preparation of this target, and the apparatus had not been cleaned thoroughly enough to remove all of the lithium. The lithium in the target proved to

Figure 7

NEUTRON YIELD FROM THE ^{7}Li (p,n) ^{7}Be AND ^{13}C (p,n) ^{13}N REACTIONS

The ^{13}C occurred in its usual abundance in the unenriched sodium cyanide target. The lithium was probably present as a contaminant inadvertently introduced during the evaporation of the target.

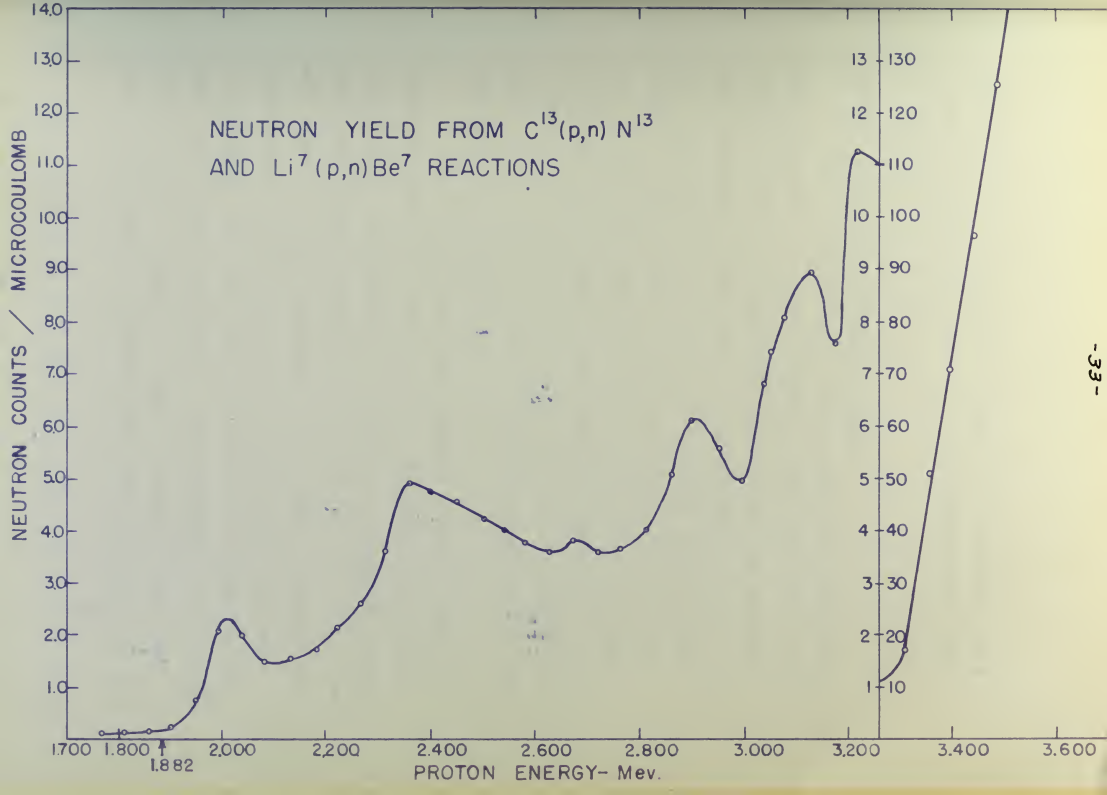
NEUTRON YIELD FROM $C^{13}(p,n)N^{13}$
AND $Li^{7}(p,n)Be^{7}$ REACTIONS
NEUTRON COUNTS / MICROCOULOMB
PROTON ENERGY- Mev.
1.882
1.700
1.800
2.000
2.200
2.400
2.600
2.800
3.000
3.200
3.400
3.600
1.0
2.0
3.0
4.0
5.0
6.0
7.0
8.0
9.0
10.0
11.0
12.0
13.0
14.0
10
20
30
40
50
60
70
80
90
100
110
120
130

be fortunate as it provided a number of well-defined peaks by which the neutron yield over a period of bombardment could be checked.

First Enriched Sodium Cyanide Target.

A thin target (3 Kev at proton energy of 1.165 Mev) of NaCN enriched in C^{14} was prepared by Baird Associates by the method described in Chapter II. This target was bombarded with an average proton beam of 5 microamperes at proton energies from 0.975 Mev to 2.500 Mev. The plot of the neutron yield vs. proton energy is shown in Figure 8 by the solid line. Since this target exhibited a large number of sharp narrow resonances above a proton energy of about 1.64 Mev the target was believed to be contaminated with some heavier element. Dr. Preston of the Shielding Group suggested that the most likely contamination was Cl^{37}.

A thin target of NaCl was prepared by Baird Associates and the neutron yield investigated by Schoenfeld and Duborg (Sc51) using the Rockefeller generator as a source of protons. Since the threshold energies of Na^{23} (Wh39) and Cl^{35} (Wh41) were well above the proton energies used, they did not enter into the reaction. Their results are shown plotted to the same proton energy scale but different neutron yield scale in the upper right corner of Figure 8. The coincidence in the proton energies of the resonances is such as to leave little doubt that the NaCN target was contaminated with chlorine. The con-

Figure 8

$^{14}C(p,n)^{14}N$ REACTION WITH ^{37}Cl CONTAMINANT vs PROTON ENERGIES OF 0.975 MEV TO 2.200 MEV

FIRST ENRICHED NaCN TARGET

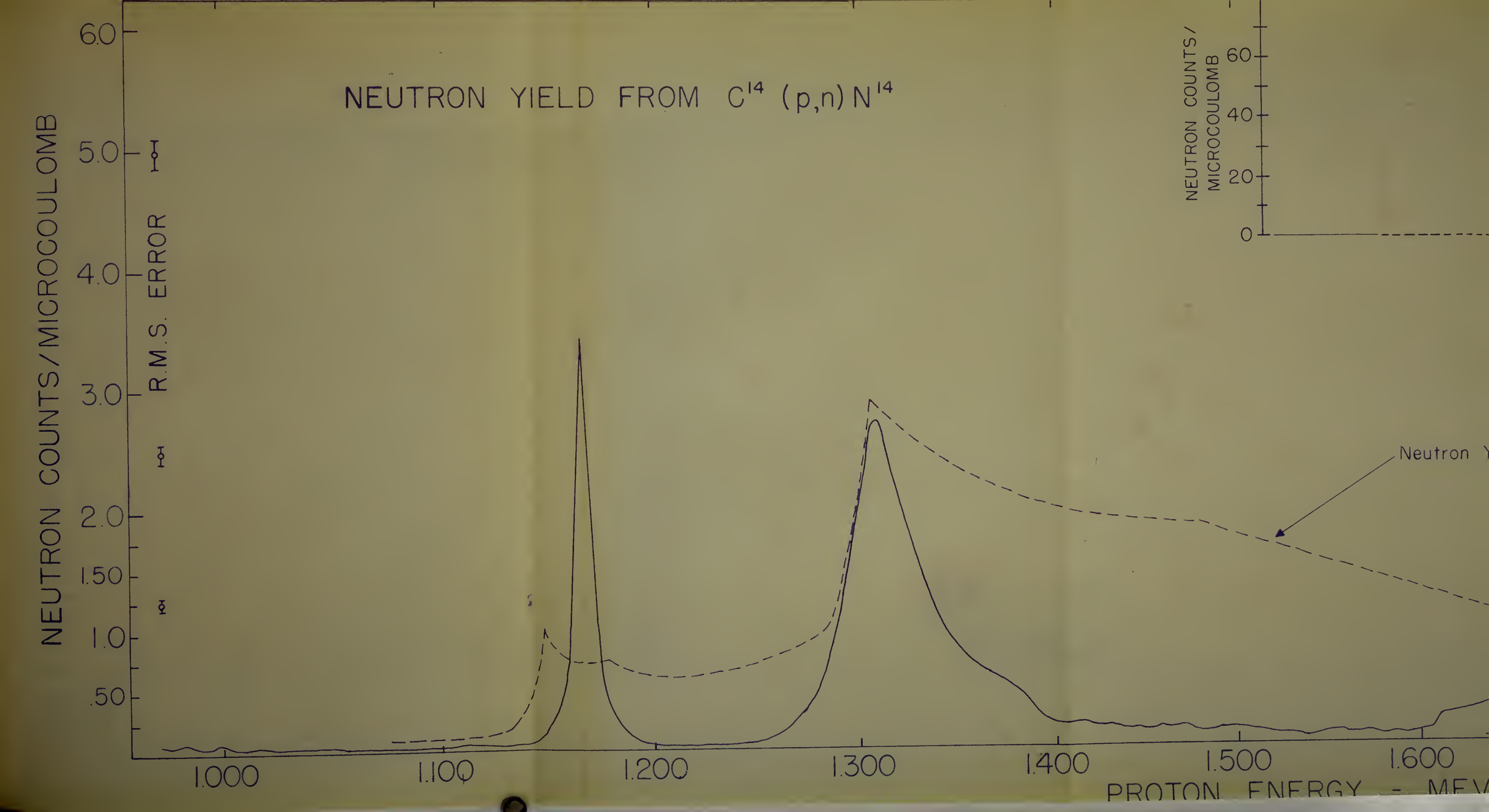
NEUTRON YIELD FROM C^{14} (p,n) N^{14}
NEUTRON COUNTS/MICROCOULOMB
R.M.S. ERROR
6.0
5.0
4.0
3.0
2.0
1.50
1.0
.50
1.000
1.100
1.200
1.300
1.400
1.500
1.600
PROTON ENERGY - MEV
NEUTRON COUNTS/ MICROCOULOMB
60
40
20
0
Neutron Y

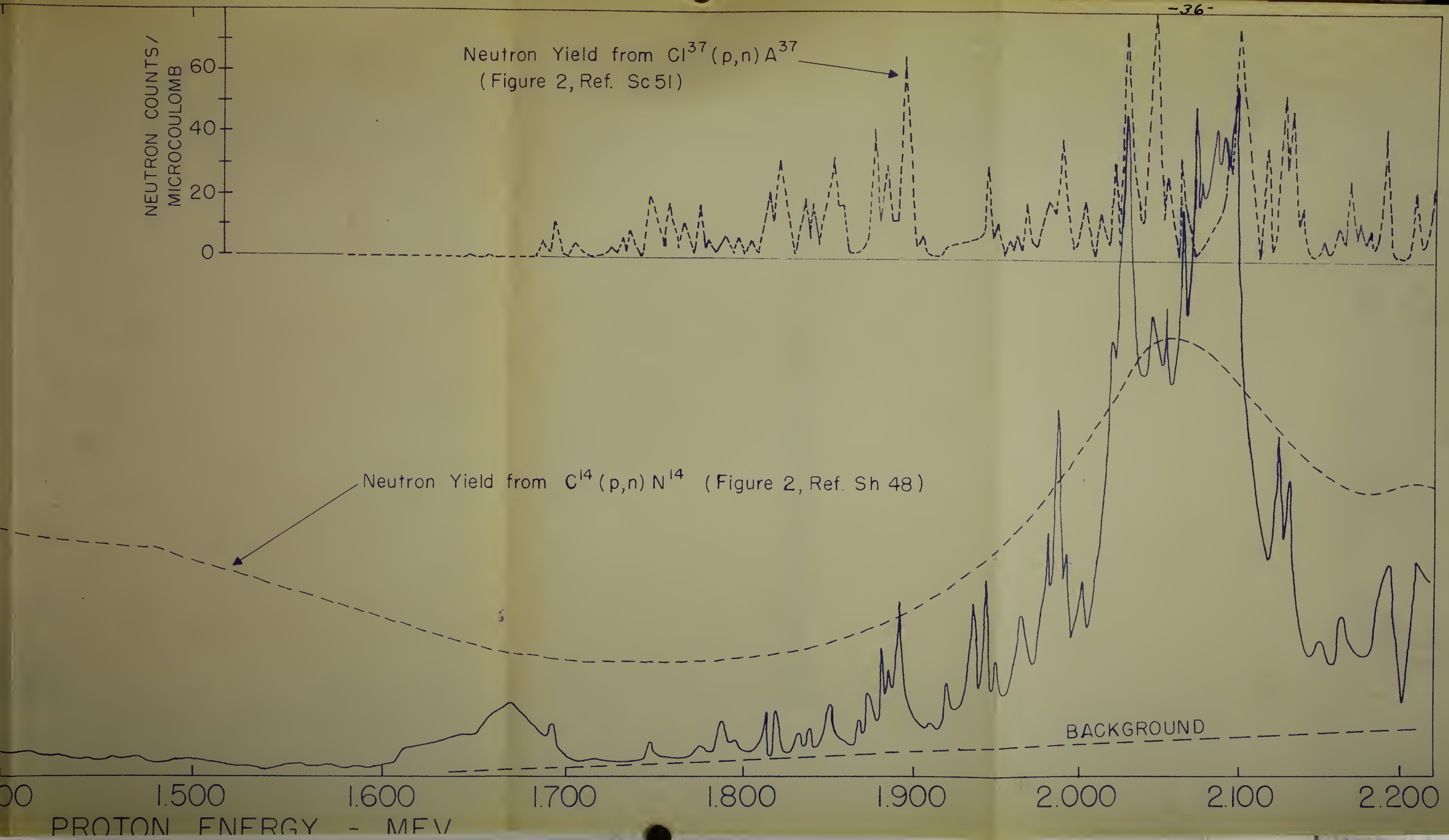
NEUTRON COUNTS/ MICROCOULOMB
0
20
40
60
Neutron Yield from Cl37 (p,n) A37
(Figure 2, Ref. Sc 51)
Neutron Yield from C14 (p,n) N14 (Figure 2, Ref. Sh 48)
BACKGROUND
1.500
1.600
1.700
1.800
1.900
2.000
2.100
2.200
PROTON ENERGY - MEV

tamination was so severe that determination with certainty of any resonances in C^{14} above a proton energy of about 2.15 Mev was impossible. However, as in the case of lithium contamination in the unenriched NaCN target, the chlorine contamination served a useful purpose. A well-defined chlorine resonance served to determine the maximum thickness of the target from which the width of the C^{14} resonance at a proton energy of 1.165 Mev was calculated.

This resonance width was determined by a method described by Fowler et al. (Fo48). The observed width at half-maximum of Cl^{37} resonances is approximately 2 Kev at 1.875 Mev proton energy. This sets a limit of 2 Kev on the maximum target thickness at this energy which is corrected to 3 Kev at the 1.165 Mev of the C^{14} resonance. The measured value of the width at half-maximum is $\Gamma' = 8.5$ Kev. The true width of the energy level, Γ, is

$$(5) \quad \Gamma = \sqrt{(\Gamma')^2 - (\Xi_t)^2} = \sqrt{(8.5)^2 - (3)^2} = 8.0 \text{ Kev.}$$

By use of the neutron yield ratio, the thickness of subsequent C^{14} targets was determined. This will be discussed in greater detail under the results obtained with subsequent targets.

Investigation of the target preparation technique and equipment indicated that it was unlikely that the contamination occurred during the target preparation. Tracerlab was notified that the NaCN supplied by them was contaminated with

what appeared to be chlorine. They agreed to investigate immediately, although they were quite certain that the contamination was not due to their processing but was probably in the material supplied to them by Oak Ridge. In order to check the efficacy of their purification technique Tracerlab first supplied a quantity of ordinary NaCN which had been deliberately contaminated with chlorine and then purified. A thin target was prepared in the usual manner by Baird Associates and bombarded in the region of proton energies between 1.960 Mev and 1.990 Mev in 1 Kev steps. The neutron yield in this region showed no resonances hence this technique for the elimination of chlorine was considered successful. Tracerlab then proceeded with the purification of the enriched NaCN.

The neutron yield from the $C^{14}(p,n)N^{14}$ reaction obtained by Shoupp et al. (Sh47) is shown by a dashed line on Figure 8 for comparison. The coincidence in proton energies of the resonances is fair except for the first which differs by 25 Kev. This may be partially explained by the lack of resolving power of the experimental method of Shoupp et al. Their location and yield of the first resonance peak was based essentially on one point, and a width at half-maximum of 40 ± 10 Kev for this resonance may be subject to considerable error as no experimental points were obtained along the sides of the resonance in the vicinity of half-maximum. A resonance width of this size does not seem consistent with the 3 Kev target reported unless there was a considerable spread in proton energies, which

there very well may have been. This width of 40 ± 10 Kev compares with the 8 Kev width at half-maximum for the first resonance found in the present experiments. This resonance is shown to an expanded proton energy scale with experimental points in part A of Figure 9. The neutron yield in the proton energy region from 1.870 Mev to 2.150 Mev is shown to an expanded energy scale in part B of Figure 9. Experimental points are not shown as they were taken at proton energy intervals of 1 to 2 Kev and were connected by straight lines with no attempt at fairing the curves.

Second Enriched Sodium Cyanide Target.

A second target of approximately the same thickness as the first target was prepared from the purified NaCN enriched in C^{14} by the same method used in the previously described targets. This target was bombarded with an average proton beam of 5 microamperes and energies from 1.065 Mev to 2.45 Mev. The neutron yield vs. proton energy plot is shown in Figure 10. Although the resonance at about 1.115 Mev found by Hinchey and Stelson (Hi51) in the N^{14} (n,a) reaction could not be verified with this target it was thought that with the higher neutron yield from a thicker target it might be found. Therefore its location is indicated as No. 1 and the first resonance found in these experiments is actually shown as No. 2.

The No. 2 resonance, whose maximum occurs at a proton energy of 1.165 Mev, is very narrow and well-defined, and has

Figure 9

NEUTRON YIELD FROM THE $C^{14}(p,n)N^{14}$ REACTION WITH Cl^{37} CONTAMINANT vs. PROTON ENERGIES OF 1.155 MEV TO 1.175 MEV AND 1.870 MEV TO 2.150 MEV

FIRST ENRICHED NaCN TARGET

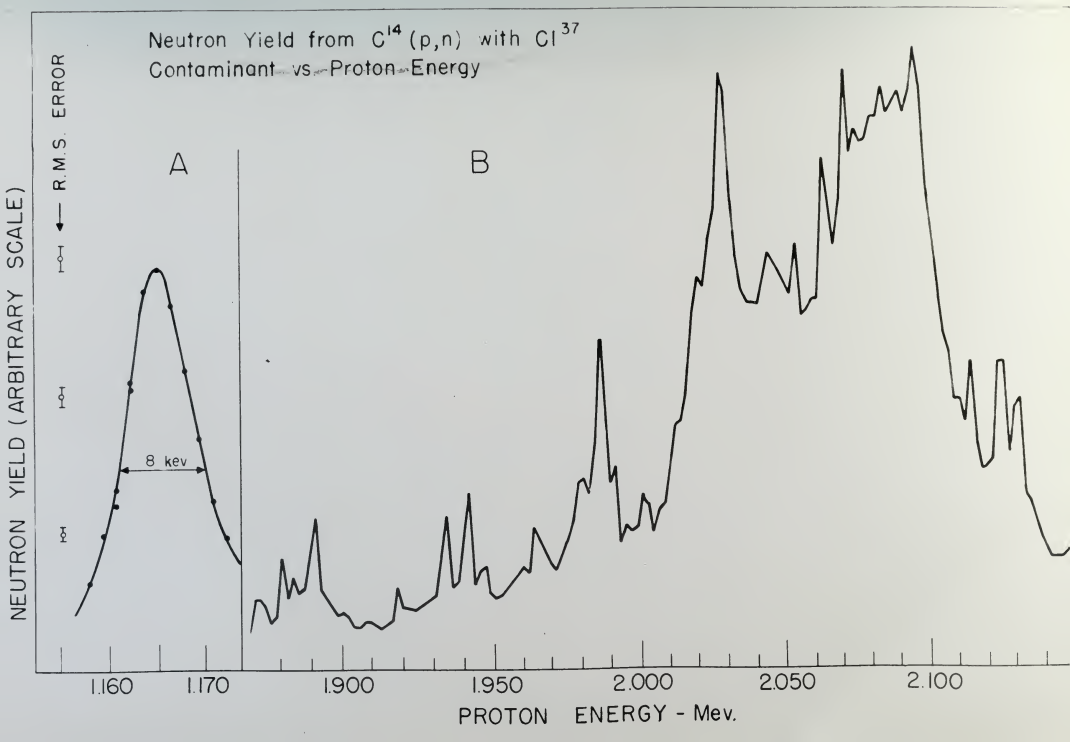
Neutron Yield from C^{14} (p,n) with Cl^{37}
Contaminant vs Proton Energy
A
B
R.M.S. ERROR
8 kev
NEUTRON YIELD (ARBITRARY SCALE)
1.160
1.170
1.900
1.950
2.000
2.050
2.100
PROTON ENERGY - Mev.

Figure 10

NEUTRON YIELD FROM THE $C^{14}(p,n)N^{14}$ REACTION vs.

PROTON ENERGIES OF 1.06 MEV TO 2.45 MEV.

SECOND ENRICHED NaCN TARGET

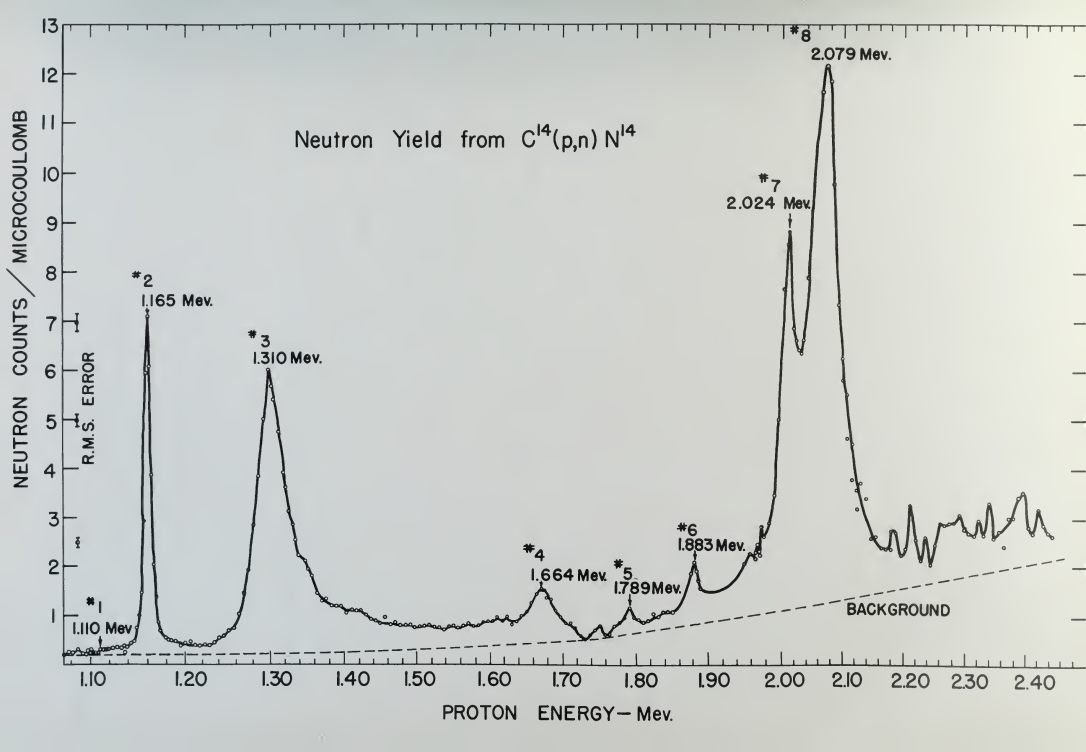
Neutron Yield from $C^{14}(p,n)N^{14}$
NEUTRON COUNTS / MICROCOULOMB
R.M.S. ERROR
PROTON ENERGY — Mev.
#1
1.110 Mev.
#2
1.165 Mev.
#3
1.310 Mev.
#4
1.664 Mev.
#5
1.789 Mev.
#6
1.883 Mev.
#7
2.024 Mev.
#8
2.079 Mev.
BACKGROUND

a true width at half-maximum of 8 Kev. The No. 3 resonance, whose maximum occurs at a proton energy of 1.310 Mev, while much broader than the preceding one, is nevertheless, quite well-defined and has a true width at half-maximum of 41 Kev. The widths of these resonances at half-maximum were calculated by the method described in the discussion of the first enriched NaCN target. Since the experimental set-up was the same for all targets and since the neutron yield at the No. 2 resonance (E_r = 1.165 Mev) was the same for both the first and second enriched targets, they were assumed to have the same thickness. The measured width at half-maximum was 8.5 Kev which, when corrected for target thickness, gave the same resonance width, 8 Kev, found in the first enriched target. In like manner the width at half-maximum of resonance No. 3 (E_r = 1.310 Mev) was measured to be 41.4 Kev which reduced to a true Γ of 41 Kev when corrected for the target thickness at this energy. These resonances are shown plotted to a much larger energy scale in Figure 11.

Weak C^{14} resonances occur at about 1.664 Mev, 1.789 Mev, and 1.883 Mev, as well as the strong ones at about 2.024 Mev and 2.079 Mev. Sufficient Cl^{37} contamination remained in the NaCN to obscure the C^{14} resonances at about 2.272 Mev and 2.451 Mev.

The background for this run is quite low and very steady. It was obtained during the run by closing the flap valve just ahead of the target, thereby intercepting the proton beam, but permitting the counter to measure the neutron background at the time and under the conditions existing during the run on the target.

Figure 11

NEUTRON YIELD FROM THE C^{14} (p,n) N^{14} REACTION IN VICINITY OF RESONANCES WHOSE MAXIMUM VALUES OCCUR AT 1.165 MEV AND 1.310 MEV.

SECOND ENRICHED NaCN TARGET

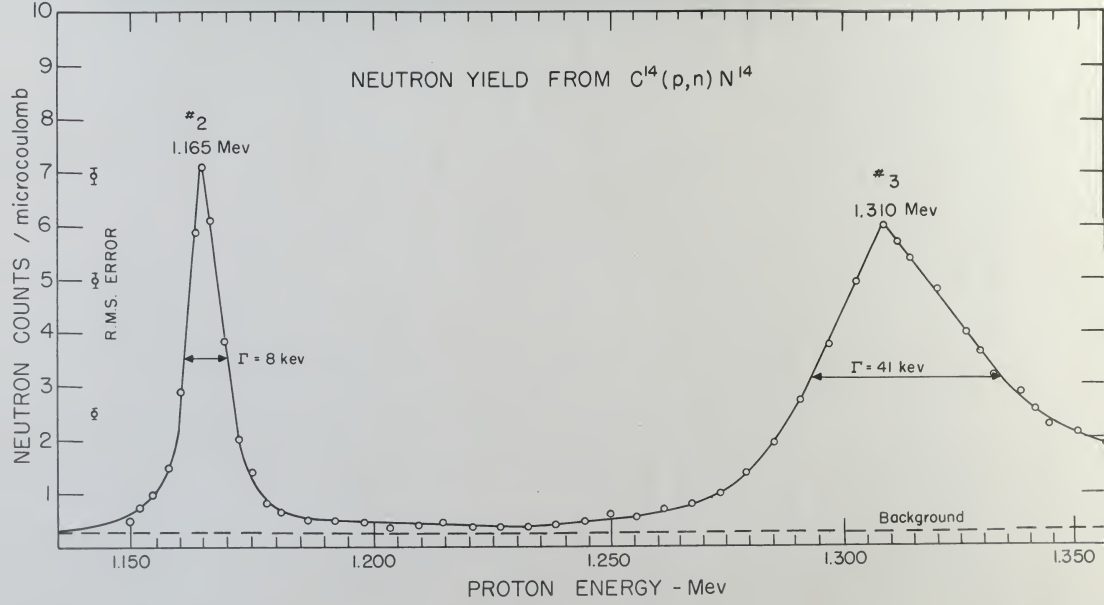
NEUTRON YIELD FROM $C^{14}(p,n)N^{14}$
#2
1.165 Mev
#3
1.310 Mev
Γ = 8 kev
Γ = 41 kev
Background
R.M.S. ERROR
NEUTRON COUNTS / microcoulomb
PROTON ENERGY - Mev
10
9
8
7
6
5
4
3
2
1
1.150
1.200
1.250
1.300
1.350

Third Enriched Sodium Cyanide Target.

A third target of approximately three times the thickness of the first two targets of enriched NaCN was prepared in a like manner. This target was bombarded with an average proton beam of 5 microamperes and energies from 1.16 Mev to 3.15 Mev. The results are plotted in Figure 12, and the energy, amplitude and width at half-maximum of the resonances are tabulated in Table II. The calculations of resonance widths and target thicknesses are summarized in Table III.

Since it was believed that all the resonances had been found in the two previous runs with thin targets, the neutron yield was measured at intervals of 7 to 8 Kev except in the region of known or suspected resonances. In these regions, points were obtained at intervals of 2 Kev or less. A total of nine resonances in this energy range were found. Repeated efforts to locate the resonance at about 1110 Kev, (shown as resonance No.1) found by Hinchey and Stelson (Hi51) in the $^{14}N(n,n)^{14}N$ reaction were unsuccessful. Resonance curves computed by the Breit-Wigner formula are shown by dotted lines for resonances No. 2 and No. 3 for comparison. These curves were computed by equation (4) on page 4:

$$(4) \quad \sigma = \pi \lambda^2 (2\ell + 1) G_J^{\ell} \frac{\Gamma_p^{\ell} \Gamma_n}{(E - E_R)^2 + \frac{\Gamma^2}{4}} .$$

At resonance ($E = E_R$) the maximum cross-section (or neutron yield) will be:

Figure 12

NEUTRON YIELD FROM THE $C^{14}(p,n)N^{14}$ REACTION

vs. PROTON ENERGY OF 1.15 Mev TO

2.60 Mev.

THIRD ENRICHED NaCN TARGET

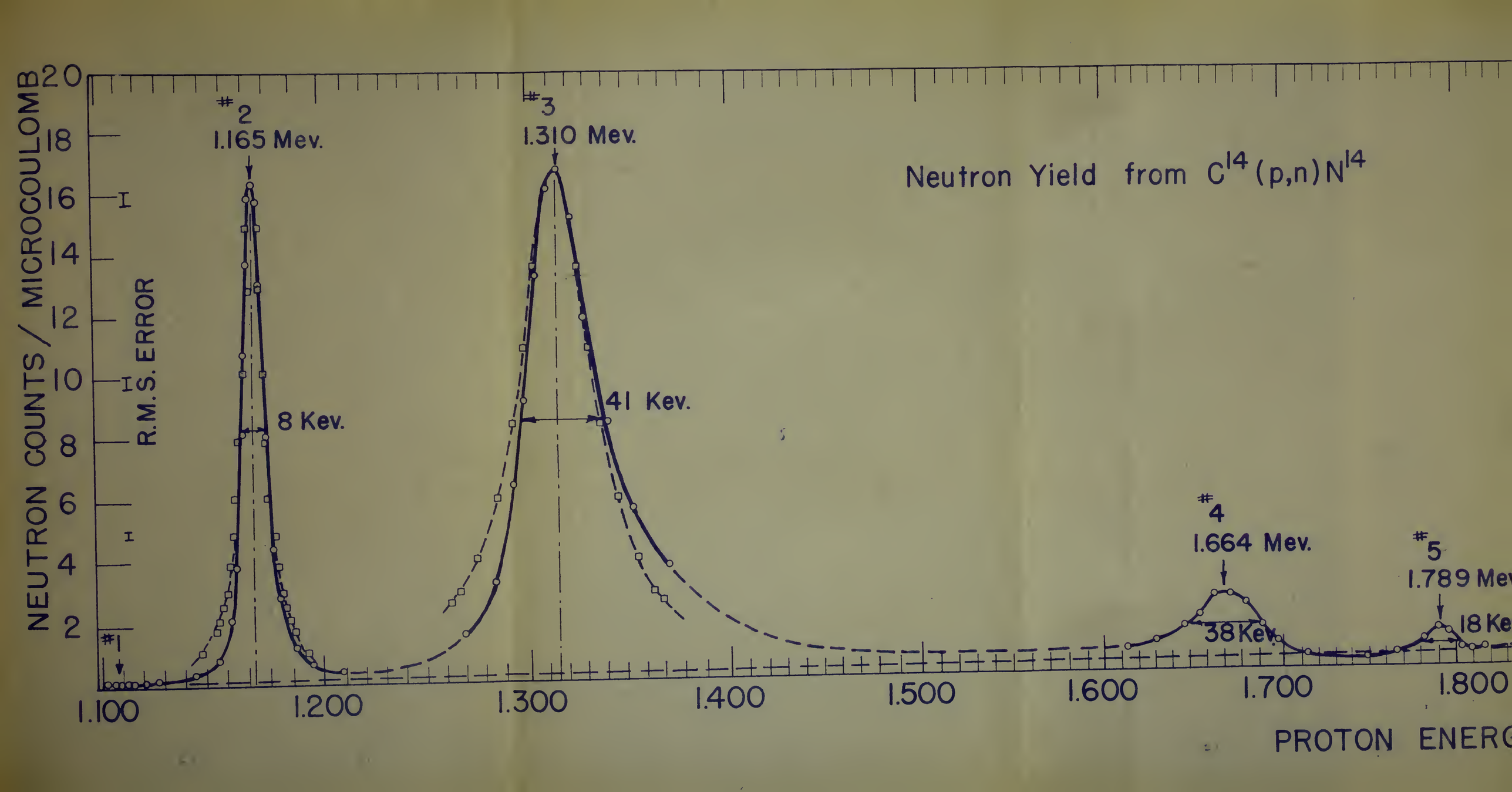
Neutron Yield from $C^{14}(p,n)N^{14}$
NEUTRON COUNTS / MICROCOULOMB
R.M.S. ERROR
#1
#2
1.165 Mev.
8 Kev.
#3
1.310 Mev.
41 Kev.
#4
1.664 Mev.
38 Kev.
#5
1.789 Mev
18 Ke
20
18
16
14
12
10
8
6
4
2
1.100
1.200
1.300
1.400
1.500
1.600
1.700
1.800
PROTON ENERG

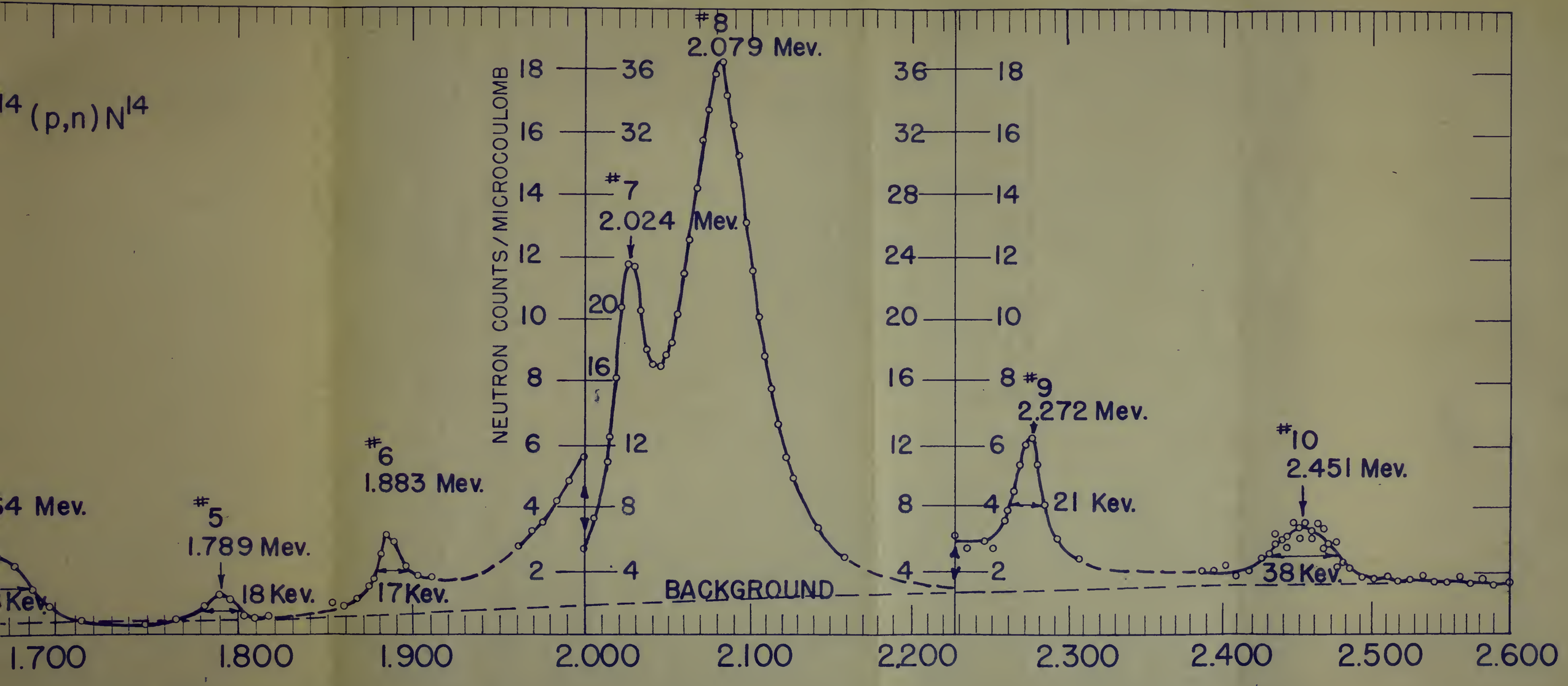
$^{14}(p,n)N^{14}$
#8
2.079 Mev.
#7
2.024 Mev.
#6
1.883 Mev.
#5
1.789 Mev.
#9
2.272 Mev.
#10
2.451 Mev.
4 Mev.
Kev.
18 Kev.
17 Kev.
21 Kev.
38 Kev.
BACKGROUND
NEUTRON COUNTS/MICROCOULOMB
18 36 16 32 14 28 12 24 10 20 8 16 6 12 4 8 2 4
1.700 1.800 1.900 2.000 2.100 2.200 2.300 2.400 2.500 2.600
PROTON ENERGY— Mev.

(6) $\sigma_{max} = \pi \lambda^2 (2\ell + 1) G_J^{\ell} \frac{\Gamma_p^{\ell} \Gamma_n}{\Gamma^2/4}$ and the

cross-section (or neutron yield) for a proton energy near resonance will be

(7) $\sigma = \frac{\sigma_{max} \Gamma^2/4}{(E - E_R)^2 + \frac{\Gamma^2}{4}} = \frac{\sigma_{max}}{\frac{(E - E_R)^2}{\Gamma^2/4} + 1} = \frac{\sigma_{max}}{\Delta^2 + 1}$ where

(8) $\Delta^2 = \frac{(E - E_R)^2}{\Gamma^2/4}$

The Γ used in these computations is the true Γ obtained from the experimentally measured Γ' corrected for the target thickness at the proton energy of the resonance by equation (5) on page 37:

(5) $\Gamma = \sqrt{(\Gamma')^2 - (E_t)^2}$.

The coincidence of the Breit-Wigner curve with the experimental curve for resonance No. 2 should be noted.

The resonances marked No. 7 and No. 8 on Figure 12 are shown to a larger energy scale in Figure 13. It is believed that these resonances are so close together that the neutron yield obtained for No. 7 is actually augmented by that of No. 8, while on the contrary, No. 8 is influenced very little by No. 7. In order to obtain a truer picture of the yield and width at half-maximum of resonance No. 7, the low energy side of No. 8 resonance is drawn symetrical with the high energy

Figure 13

NEUTRON YIELD FROM THE $C^{14}(p,n)N^{14}$ REACTION vs.

PROTON ENERGY OF 1.950 Mev to 2.200 Mev.

THIRD ENRICHED NaCN TARGET

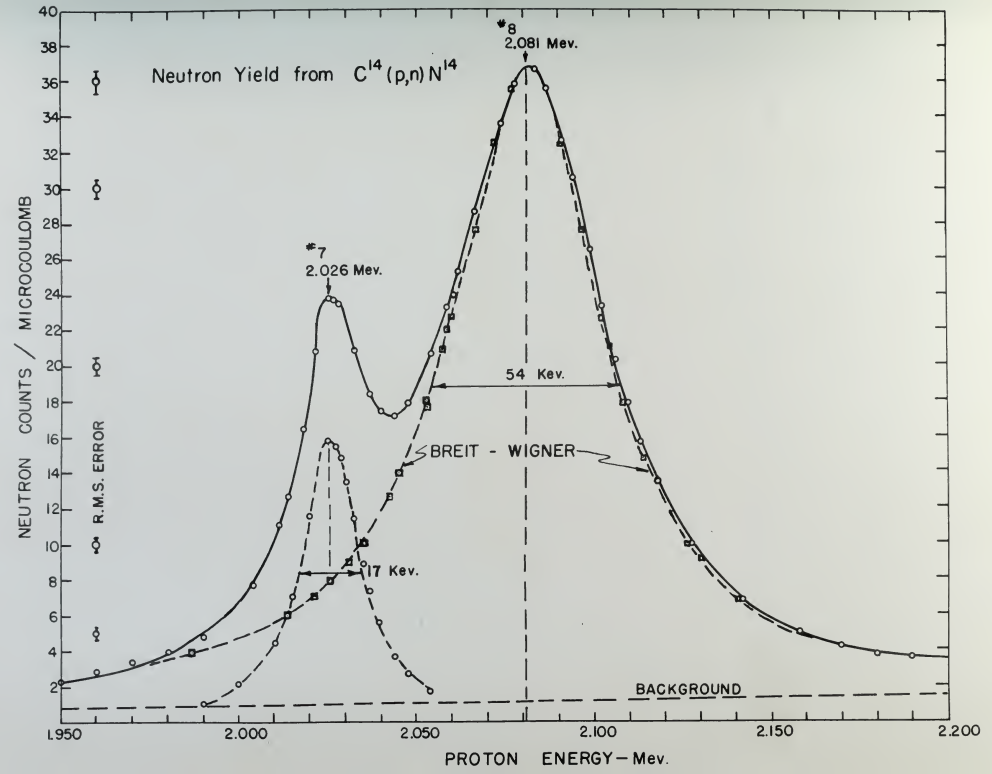
Neutron Yield from $C^{14}(p,n)N^{14}$
#8
2.081 Mev.
#7
2.026 Mev.
54 Kev.
BREIT - WIGNER
17 Kev.
BACKGROUND
NEUTRON COUNTS / MICROCOULOMB
R.M.S. ERROR
PROTON ENERGY — Mev.
1.950
2.000
2.050
2.100
2.150
2.200

side which is practically coincident with the Breit-Wigner curve for this resonance. The contribution of No. 8 to the yield of No. 7 is then subtracted from the measured yield of No. 7 and a new resonance curve for No. 7 is shown beneath it. This resonance is almost identical in shape with one computed using the Breit-Wigner formula, equations (4), (5), (6), (7), and (8) above.

Table II

The proton energies of the resonance peaks, E_r, are determined from the plot of the experimental points. The target thickness, E_t, at the energy of resonance No. 2, is determined from the Γ' for this resonance (previously determined in the first and second targets) by the relation $E_t = \sqrt{(\Gamma')^2 - (\Gamma)^2}$. The target thickness at the proton energies of the other resonances is determined by applying a correction factor (shown in Table III) obtained from Figure 12, Appendix B. The proton energies of the resonances corrected for target thickness, E_{rt}, are obtained by subtracting half the target thickness, E_t, from the measured resonance peak energy, E_r. The Γ's are determined from the plot of experimental points. The Γs are obtained from Γ' and E_t by equation (5), $\Gamma = \sqrt{(\Gamma')^2 - (E_t)^2}$. The neutron yields at resonance, Y, are obtained from the experimental plot. The excitation energies of levels in N^{15} are obtained by adding the proton energies of the resonances, E_{rt}, corrected to center of mass system by multiplying by (14/15), to energy level of C^{14} + p, 10.207 Mev above the ground level of N^{15}.

TABLE II

Proton Energy, neutron yield, target thickness, and width at half-maximum amplitude of resonances found in the third NaCN enriched target

E_r - Proton Energy at resonance peak maximum

E_t - Target Thickness

E_{rt} - Proton Energy of resonance corrected for target thickness

Γ' - Measured resonance width at half-maximum

Γ - Energy level width at half-maximum

Y - Neutron yield per microcoulomb at resonance peak

E_x - Excitation energy of levels in N^{15}

Resonance No.	E_r		E_t	E_{rt}	Γ'		Γ	Y	E_x
	Mc	Mev	Kev	Mev	Kc	Kev	Kev		Mev
2	8.260	1.169	8.0	1.165	40	11.3	8	16.1	11.29
3	8.754	1.314	7.2	1.310	140	42.0	41	16.5	11.43
4	9.862	1.667	6.0	1.664	114	38.4	38	2.0	11.76
5	10.226	1.792	5.7	1.789	53	18.6	18	0.8	11.88
6	10.492	1.886	5.5	1.883	50	17.9	17	2.3	11.96
7	10.900	2.027	5.2	2.024	48	18.0	17	14.9	12.10
8	11.022	2.081	5.1	2.079	142	54.0	54	35.6	12.15
9	11.520	2.274	4.7	2.272	54	21.4	21	4.3	12.33
10	11.970	2.453	4.4	2.451	94	38.6	38	1.7	12.49

TABLE III

Calculation of Target Thickness and Resonance Widths at Half-Maximum

$$\Gamma = \sqrt{(\Gamma')^2 - (E_t)^2}$$

Resonance No.	Proton Energy E_r - Kev.	Measured Resonance Width Γ' - Kc.	Conversion Factor Kev/Kc.	Measured Resonance Width at Half-Maximum Γ' - Kev.	Target Thickness at E_r=1165 Kev. E_t - Kev	Target Thickness Energy Correction Factor	Target Thickness at Resonance E_t - Kev.	Resonance True Width at Half-Maximum Γ - Kev.
2	1165	40	0.283	11.3	8.0	1	8.0	8.0
3	1310	140	0.300	42	8.0	0.9	7.2	41.4
4	1664	114	0.337	38.4	8.0	0.76	6.0	37.9
5	1789	53	0.351	18.6	8.0	0.72	5.7	17.7
6	1883	50	0.358	17.9	8.0	0.69	5.5	17.1
7	2026	48	0.372	18.0	8.0	0.65	5.2	17.2
8	2079	142	0.379	54.0	8.0	0.63	5.1	53.7
9	2272	54	0.396	21.4	8.0	0.59	4.7	20.9
10	2451	94	0.410	38.6	8.0	0.55	4.4	38.2

CHAPTER V

CONCLUSIONS

The same energy levels in the compound nucleus N^{15} can be excited by different reactions, $C^{14}(p,n)N^{14}$, $N^{14}(n,p)C^{14}$, $N^{14}(n,\alpha)B^{11}$. It is expected that the resonances in the yields of the reactions $C^{14}(p,n)N^{14}$ and $N^{14}(n,p)C^{14}$ will occur at energies differing by the $C^{14}(p,n)N^{14}$ threshold, E_t = 671 Kev (To 50). The positions of the resonances obtained in this experiment are compared with those obtained by others in Table IV.

The agreement of this work with that of Hinchey and Stelson (Hi50) on the $N^{14}(n,p)C^{14}$ reaction, done concurrently here at M.I.T. is excellent. It should be noted in Table IV that all nine resonances found in each work are in agreement within the experimental errors, which, in each case, are quite small. In addition to this excellent agreement, three resonances, not previously reported in the literature, were found in both investigations.

The agreement of these experiments with those of Johnson and Barschall (Jo50) is also excellent and the four resonances reported by them are in agreement within the experimental errors. The smaller experimental errors, especially in the case of resonance No. 8, is noteworthy. The (p,n) yield curve, Figure 12 of this work, is quite similar to the (n,p) yield curve, Figure 3, in Johnson and Barschall.

In comparing this work with that of Stebler and Huber (St48), the four resonances they determined are in agreement within the experimental errors, but their large experimental errors should be noted.

None of the three resonances found by Barschall and Battat (Ba46) is in agreement, however, they listed no experimental errors.

In comparison with the C^{14} (p,n) work of Shoupp et al. (Sh48) it is noted that only one of the six resonances they reported are in agreement, inspite of their rather large experimental errors.

A partial energy level diagram for N^{15} in the region between approximately 11 to 12.5 Mev above the ground state is shown in Figure 14. It is believed to be much more complete and accurate in the region covered than that shown in Hornyak, Lauritsen, Morrison and Fowler (Ho50). The most accurate value of the neutron binding energy in N^{15} is believed to be 10.833 ± .007 Mev according to Li et al. (Li51). This value establishes the level for N^{14} + n, and by subtracting the C^{14} (p,n) threshold value of 0.671 Mev the C^{14} + p level is determined to be 10.207 Mev above the ground level of N^{15}.

TABLE IV

Positions of Resonances in the $C^{14}(p,n)N^{14}$ Reaction Expressed in Terms of Proton Energies, E_p, in Kev. $E_p = E_n + E_t = E_n + 671$ Kev. (Resonances Reported as doubtful are enclosed in parentheses.)

Resonance No.	This Experiment (n,p) E_p	Hinchey and Stelson (H151) (n,p) $E_n + 671$	Johnson and Barschall (Jo50) (n,p) and (n,α) $E_n + 671$	Stebler and Huber (St48) (n,p) and (n,α) $E_n + 671$	Barschall and Battat (Ba46) (n,p) $E_n + 671$	Shoupp et al. (Sh48) (p,n) E_p
1		1115 ± 3				
2	1165 ± 2	1165 ± 4	1170 ± 5	1151 ± 50	1221	1140 ± 20
3	1310 ± 3	1314	1311 ± 7	1311 ± 40	1371	1300 ± 20
4	1664 ± 4	1663	(1664 ± 12)			(1470 ± 50)
5	1789 ± 4	1791 ± 4				
6	1883 ± 4	1883 ± 4				
7	2024 ± 5	2020				
8	2079 ± 5	2074	2086 ± 50	2081 ± 90	2121	2050 ± 20
9	2272 ± 6	2268 ± 4				(2210 ± 50)
10	2451 ± 10	2453 ± 6	2471 ± 15	2441 ± 110		
11						(2650 ± 50)

Figure 14

PARTIAL ENERGY LEVEL DIAGRAM FOR N^{15}

The proton energies of the resonances, E_p, shown in the C^{14} + p section are in the laboratory system and when corrected to the center of mass system and added to the ground level energy of C^{14} + p (10.207 Mev above ground level of N^{15}) give the energy levels of N^{15}.

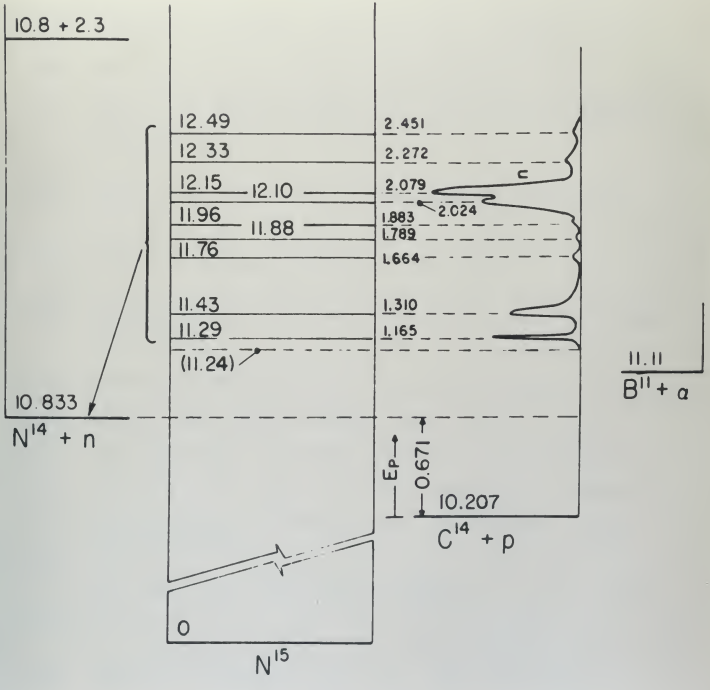
10.8 + 2.3
12.49
12 33
12.15
12.10
11.96
11.88
11.76
11.43
11.29
(11.24)
10.833
N14 + n
2.451
2.272
2.079
c
2.024
1.883
1.789
1.664
1.310
1.165
11.11
B11 + a
Ep
0.671
10.207
C14 + p
0
N15

BIBLIOGRAPHY

Ad50 R.E. Adamson, M.S. Thesis, "A Study of Excited States of N^{14} from the $C^{13}(p,n)N^{13}$ Reaction," MIT (1950).

Ba46 Barschall and Battat, Phys. Rev. 70, 245 (1946).

Ba50 Baker and Howell, MIT M.S. Thesis (1950).

Bl50 Blatt, J.M. and Weisskopf, V.F., "The Theory of Nuclear Reactions," Technical Report No. 42, L.N.S.E., MIT (May, 1950).

El49 Elmore, W.C. and Sands, M., Electronics, McGraw-Hill, 1949.

Fo48 Fowler, W.A. et al., RMP 20, 236 (1948).

Gu47 Guggenheimer, Heitler and Powell, Proc. Roy. Soc. A 190, 196 (1947).

Ha47 Hanson and McKibben, Phys. Rev. 72, 673 (1947).

Ha51 Hadden, F.A., MIT PhD Thesis (Feb., 1951).

He37 Herb, Parkinson and Kerst, Phys. Rev. 51, 75 (1937).

He49 Herb, Phys. Rev. 75, 246 (1949); Ibid 76, 502 (1949).

Hi51 Hinchey, J.J. and Stelson, P.H., MIT Personal Communication, 1951.

Ho50 Hornyak, W.F., Lauritsen, T., Morrison, P., and Fowler, W.A., Rev. Mod. Phys. 22, 291 (1950).

Hu48 Hughes and Eggler, Phys. Rev. 73, 809 (1948).

Jo50 Johnson and Barschall, Phys. Rev. 80, 818 (1950).

Ki50 Kinsey, Bartholomew, and Walker, Phys. Rev. 77, 723 (1950).

BIBLIOGRAPHY (continued)

Li51 Li, Whaling, Fowler and Lauritsen, private communication to W.W. Buechner (1951).

Ma50 Malm, R. and Buechner, W.W., Phys. Rev. 80, 771 (1950).

Sc51 Schoenfeld, W.A. and Duborg, R.W., MIT M.S.Thesis (1951).

Sh48 Shoupp, Jennings, and Sun, Phys. Rev. 75, 1 (1949).

St47 Stephens, Spruch and Schiff, University of Pennsylvania Report, (June, 1947).

To50 Tollestrup, A., Fowler, W.A., and Lauritsen, C.C., "Nuclear Mass Determinations from Nuclear Q Values," Phys. Rev. 78, 372 (1950).

Tu35 Tuve, Hafstad, and Dahl, Phys. Rev. 48, 315,(1935).

Va31 Van de Graaff, Phys. Rev. 38, 1919 (1931).

Va33 Van de Graaff, Compton and Van Atta, Phys. Rev. 43, 149 (1933).

Va48 Van de Graaff, Trump and Buechner, Reports on Progress in Physics, Vol. XI, 1 (1948), The Physical Society, Great Britain.

Wa49 Walker, R.L., Phys. Rev. 76, 244 (1949).

Wh39 White, M.G., Phys. Rev. 56, 512 (1939).

Wh41 White, M.G., Phys. Rev. 59, 63 (1941).

Wi50 Willard, H.B., Preston, W.M., and Goodman, C., "The Interaction of Fast Neutrons with Nuclei," Technical Report No. 45, L.N.S.E., MIT (Sept., 1950).

Wy49 Wyly, L.D., Phys. Rev. 76, 316 (1949).

ACKNOWLEDGMENTS

The graduate study of the author was sponsored by the Bureau of Ships and the U.S. Naval Postgraduate School. The work reported herein was undertaken in conjunction with the Nuclear Shielding Project of the Laboratory of Nuclear Science and Engineering, M.I.T., which project is sponsored by the Bureau of Ships and the Office of Naval Research.

The author wishes to express his appreciation to Professor Clark Goodman for his guidance as thesis supervisor, to Dr. J.J.G. McCue for his many long hours of experimental assistance and helpful criticism, to Dr. W.M. Preston for his assistance in analysis of data as well as experimental guidance, to Messrs. D.C. Thompson and I.E. Slawson for their aid in conducting the experiments at the Rockefeller generator, to Miss Mary Abramo for typing the manuscript, and to Mr. C.W. Tourtellotte and the Drafting Department of the L.N.S.E. for their cooperation in reproducing the figures.

The cooperation of Mr. Barr of Baird Associates in preparing targets of the requested thickness and at the time desired contributed appreciably to the success of the experiments.

The prompt and efficient purification of the contaminated NaCN enriched in C^{14} by Tracerlab, Inc. is appreciated.

Appendix A - Table V - Conversion of Frequency to Energy-Kc/Kev.

Appendix B - Figure 15 - Proton Energy Loss per Unit Target Thickness vs Proton Energy.

Appendix C - Magnetic Field Regulation Using Nuclear Magnetic Resonance.

Table V Based on E_o = 1.8822 f_o = 10.480

Mo f	kev E	kev/ko ΔE
7.5	964.0	
		.259
7.6	989.9	
		.262
7.7	1016.1	
		.265
7.8	1042.6	
		.269
7.9	1069.5	
		.273
8.0	1096.8	
		.276
8.1	1124.4	
		.279
8.2	1152.3	
		.283
8.3	1180.6	
		.286
8.4	1209.2	
		.290
8.5	1238.2	
		.293
8.6	1267.5	
		.296
8.7	1297.1	
		.300
8.8	1327.1	
		.303
8.9	1357.4	
		.307
9.0	1388.1	
		.310
9.1	1419.1	
		.314
9.2	1450.5	
		.317
9.3	1482.2	
		.321
9.4	1514.3	
		.324
9.5	1546.7	
		.327
9.6	1579.4	
		.331
9.7	1612.5	
		.334
9.8	1645.9	
		.337
9.9	1679.6	
		.341
10.0	1713.7	
		.345
10.1	1748.2	
		.348
10.2	1783.0	
		.351
10.3	1818.1	
		.355
10.4	1853.6	
		.358
10.5	1889.4	
		.362
10.6	1925.6	
		.365
10.7	1962.1	
		.368
10.8	1998.9	
		.372
10.9	2036.1	
		.375
11.0	2073.6	
		.379
11.1	2111.5	
		.382
11.2	2149.7	
		.386
11.3	2188.3	
		.389
11.4	2227.2	
		.392
11.5	2266.4	
		.396
11.6	2306.0	
		.399
11.7	2345.9	
		.403
11.8	2386.2	
		.406
11.9	2426.8	
		.410
12.0	2467.8	
		.413
12.1	2509.1	
		.416
12.2	2550.7	
		.420
12.3	2592.7	
		.423
12.4	2635.0	
		.427
12.5	2677.7	
		.430
12.6	2720.7	
		.434
12.7	2764.1	
		.437
12.8	2807.8	
		.440
12.9	2851.8	
		.444
13.0	2896.2	
		.447
13.1	2940.9	
		.451
13.2	2986.0	
		.454
13.3	3031.4	
		.458
13.4	3077.2	
		.461
13.5	3123.3	
		.464
13.6	3169.7	
		.468
13.7	3216.5	
		.472
13.8	3263.7	
		.475
13.9	3311.2	
		.478
14.0	3359.0	
		.481
14.1	3407.1	
		.485
14.2	3455.5	
		.488
14.3	3504.4	
		.492
14.4	3553.6	
		.496
14.5	3603.2	
		.499
14.6	3653.1	
		.502
14.7	3703.3	
		.505
14.8	3753.8	
		.509
14.9	3804.7	
		.512
15.0	3855.9	

FIGURE 15

PROTON ENERGY LOSS PER UNIT TARGET THICKNESS vs PROTON ENERGY

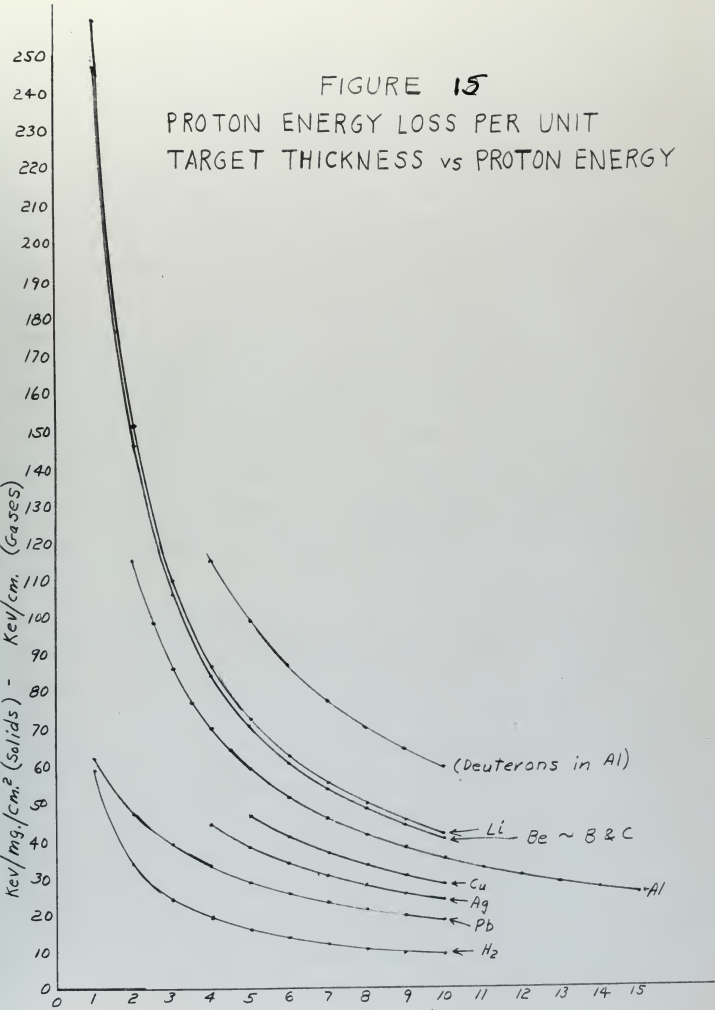

APPENDIX C

Magnetic Field Regulation Using Nuclear Magnetic Resonance

For many years the fundamental standard for measuring the strength of magnetic fields has been the voltage generated by a coil cutting a magnetic flux or a force upon a wire carrying a known current. In the case of the magnet used for deflecting the proton beam in the Rockefeller Electrostatic Generator neither of these methods is practical because insufficient space within the uniform magnetic field is not available without redesigning the chamber, and because remote control due to the high neutron flux is required. What has been needed in this case is a quantity which is readily measured with precision and which is proportional to the magnetic flux.

For this application the use of nuclear magnetic resonance is ideal. A fundamental and unchanging property of atomic nuclei is used to relate the strength of a magnetic field in which the nuclei are placed and a frequency. Atomic nuclei which have a resultant magnetic moment and angular momentum, if placed in a magnetic field, will tend to align themselves with the field. In the process of approaching this new alignment, the direction of the angular momentum vector of the nucleus must change, which results in a precession of the nucleus about the axis of the orienting magnetic field. It is the frequency of this precession which is the characteristic

that is proportional to the strength of the magnetic field. It is related by the expression $\omega_{r_o} = \gamma$Ho where ω_{r_o} is the radian frequency of this free precession, γ is known as the gyromagnetic ratio, and Ho is the strength of the field. If energy is applied to the nuclei at a frequency, ω_r, near the frequency of free precession, ω_{r_o}, precession of the nuclei is induced at the frequency ω_r. The externally manifested characteristics of the phenomenon are similar to the characteristics of any of the more familiar resonant systems.

The nuclear resonance phenomenon can be readily applied to the control of magnetic fields because a voltage can be obtained directly from the equipment used to detect the precession hereafter called resonance. This voltage is proportional to the deviation of the magnetic field, Ho, from the equivalent-reference magnetic field, Href. Href. is a fictitious field that is proportional to the square of the measured, applied, reference frequency. For a control system, the difference between the Href. and Ho is the error in the magnetic field, and hence, the voltage obtained from the nuclear resonance equipment is an error voltage. The error voltage can be used to control the current producing the magnetic flux and hence a precision magnetic field regulator can be obtained.

The use of nuclear magnetic resonance to control a magnetic field can reduce the variations in magnetic flux almost as may be desired. Nuclear resonance field control has been obtained which ranged in precision from the best results of other types of controls, ie., about one part in 30 thousand

by Buechner at M.I.T., to better than one part in a million by Bitter, Wimett and Adams at M.I.T.

The measured applied reference frequency is obtained from a Model LR-3 Combined Heterodyne Frequency Meter and Crystal Controlled Calibrator Equipment, manufactured by the General Radio Company of Cambridge, Massachusetts. This equipment has a frequency measuring range of 160 Kc to 30 Mc, and by harmonic extension, frequencies above 30 Mc may be measured. The equipment consists of a single unit which includes all power supply equipment, heterodyne frequency meter, crystal calibrator, detector-audio amplifier and interpolator (electronic frequency meter). It has an accuracy of 1 part in one hundred thousand which therefore sets the maximum accuracy of the proton resonance equipment.

For a complete description of nuclear resonance, both from the quantum mechanical point-of-view and from Newtonian physics, the reader is referred to the thesis, "Precision Magnetic Field Regulation Using Nuclear Magnetic Resonance," by F.A. Hadden, M.I.T., February, 1951, from which most of the above description was obtained. In addition to the above description, the equipment, control system, nuclear resonance parameters, and practical considerations in construction are also discussed at length.

AUG 31 BINDERY

15656
Thesis Roseborough
R76 Resonances in the C^{14} (p,n)N^{14} reaction and energy levels of N^{15}.

5656
he
ion
of

Thesis 15656
R76 Roseborough
Resonances in the C^{14} (p,n)N^{14} reaction and energy levels of N^{15}.

Library
U. S. Naval Postgraduate School
Monterey, California

SHERIDAN GOLD LETTERING AND SMITH BINDERY GLENDALE

thesR76
Resonances in the C Superscript 14 (p,n
3 2768 001 98135 0
DUDLEY KNOX LIBRARY